1 **Treatment with the neutralizing antibody against repulsive guidance**

2 **molecule-a promotes recovery from impaired manual dexterity in a**

3 **primate model of spinal cord injury**

4 **Authors:** Hiroshi Nakagawa[1,2]*, Taihei Ninomiya[1], Toshihide Yamashita[2], Masahiko

5 Takada[1]

6

7 **Affiliations:**

8 [1]Systems Neuroscience Section, Primate Research Institute, Kyoto University, Inuyama,

9 Aichi 484-8506, Japan.

10 [2]Department of Molecular Neuroscience, Graduate School of Medicine, Osaka

11 University, Suita, Osaka 565-0871, Japan.

12

13 *Corresponding author: Hiroshi Nakagawa

14 Present address for HN: Sobell Department of Motor Neuroscience and Movement

15 Disorders, Institute of Neurology, University College London, Queen Square, London,

16 WN1C 3BG, United Kingdom. Tel: 44-20-3448-4403; Fax: 44-20-7813-3107; E-mail:

17 h.nakagawa@ucl.ac.uk

18

19    Present address for TN: Department of System Neuroscience, National Institute for

20    Physiological Sciences, 38 Nishigonaka Myodaiji, Okazaki, Aichi, 444-8585, Japan.

21

22    **Running title:** RGMa is a potential molecular target for SCI.

23

24 **Keywords**

25 manual dexterity; corticospinal tract; repulsive guidance molecule-a; primates; spinal

26 cord injury

27

**Abstract**

28

29          Axons in the mature mammalian central nervous system have only a limited

30  capacity to grow/regenerate after injury, and, therefore, spontaneous recovery of motor

31  functions is not greatly expected in spinal cord injury (SCI). To promote functional

32  recovery after SCI, it is critical that corticospinal tract (CST) fibers reconnect properly

33  with target spinal neurons through enhanced axonal growth/regeneration. Here, we

34  applied antibody treatment against repulsive guidance molecule-a (RGMa) to a monkey

35  model of SCI. We found that inhibition of upregulated RGMa around the lesioned site in

36  the cervical cord resulted in recovery from impaired manual dexterity by accentuated

37  penetration of CST fibers into laminae VII and IX where spinal interneurons and

38  motoneurons are located, respectively. Furthermore, pharmacological inactivation

39  following intracortical microstimulation revealed that the contralesional, but not the

40  ipsilesional, primary motor cortex was crucially involved in functional recovery at a late

41  stage in our SCI model. The present data indicate that treatment with the neutralizing

42  antibody against RGMa after SCI is a potential target for achieving restored manual

43  dexterity in primates.

44

**Introduction**

45

46          Manual dexterity as represented by a precision grip is skilled motor behavior

47 characteristic of higher primates. It is generally accepted that manual dexterity is closely

48 related to direct connectivity of the corticospinal tract (CST) arising from the motor

49 cortex to motoneurons of the cervical cord that control the distal hand muscles (Lemon,

50 1993). The spinal cord injury (SCI) disrupts the CST and often causes an ever-lasting

51 disability with sensorimotor dysfunctions. Therefore, the CST has been focused as an

52 essential target for SCI treatment (GrandPré et al., 2002; Oudega and Perez, 2012).

53 However, the mature mammalian central nervous system (CNS) has only a limited

54 capacity to grow/regenerate once injured because of a number of inhibitory factors,

55 including axon guidance molecules (Yiu and He, 2006).

56          Repulsive guidance molecule-a (RGMa) is among the axon guidance molecules.

57 This molecule was originally identified in the visual system (Stahl et al., 1990; Monnier

58 et al., 2002), and has been implicated in neuronal survival, proliferation and

59 differentiation (Matsunaga et al., 2004; Matsunaga et al., 2006; Lah and Key, 2012).

60 RGMa was upregulated around the lesioned site after SCI in rodents (Schwab et al.,

61 2005), and treatment with the neutralizing antibody against RGMa has been shown to

62 accelerate axonal regrowth and sprouting from the CST following thoracic cord lesions

63    (Hata et al., 2006). On the other hand, to promote functional recovery by enhanced

64    sprouting of CST fibers after CNS insults, such fibers are required to extend toward an

65    appropriate locus and reconnect properly with target spinal neurons (Wahl et al., 2014). It

66    has recently been reported in macaque monkeys that a number of sprouting CST fibers

67    derived from the contralesional primary motor cortex (MI) after SCI penetrate, below the

68    lesioned site, into laminae VII and IX where spinal interneurons and motoneurons are

69    located, respectively. Moreover, the ratio of the axonal distribution was significantly

70    increased in lamina IX (Nakagawa et al., 2015). By contrast, the sprouting CST fibers

71    chiefly terminate within the medial gray matter in rodents (Hata et al., 2006; Vavrek et al.,

72    2006). These results suggest that the mechanisms underlying axonal remodeling that

73    leads to the recovery of motor functions after SCI may differ in higher primates and

74    rodents. Therefore, it is important to understand axonal remodeling specific to higher

75    primates for restoration of manual dexterity after SCI. It is also crucial to confirm

76    whether RGMa suppression promotes the recovery from impaired manual dexterity for

77    applying to human patients with SCI.

78        The present study aimed at establishing the antibody treatment against RGMa in

79    higher primates. Our results indicate that treatment with the neutralizing antibody against

80    RGMa is critical to achieve restored manual dexterity after SCI.

81                                         6

82    **Materials and Methods**

83    **Animals**

84          Twelve rhesus monkeys (*Macaca mulatta*, 3–5 years old, 3.8–5.4 kg) of either

85    sex were used in the present study: three lesioned monkeys for treatment with control

86    antibody (Ctrl-A to Ctrl-C), four monkeys for treatment with anti-RGMa antibody

87    (RGMa-A to RGMa-D), and five normal monkeys for molecular biological (western

88    blotting) and histological (histochemical, immunohistochemical, and *in situ*

89    hybridization) analyses. The experimental protocols were approved by the Animal

90    Welfare and Animal Care Committee of the Primate Research Institute, Kyoto

91    University, Japan. All experiments were conducted in accordance with the Guide for

92    Care and Use of Laboratory Primates (Ver. 3, 2010) by the Primate Research Institute,

93    Kyoto University, Japan.

94

95    **Anti-RGMa antibody**

96          We used an anti-human RGMa antibody (mouse IgG; IBL) as a neutralizing

97    antibody against RGMa in the present study. The antibody was raised against the

98    C-terminal sequences of human RGMa, LYERTRDLPGRAAAGL. The protein

99    sequence of human RGMa fully corresponds with that for macaque monkeys. It has

7

100 previously been reported that the antibody has an inhibitory effect on human RGMa

101 obtained from peripheral blood mononuclear cells of human patients with multiple

102 sclerosis (Muramatsu et al., 2011).

103

104 **Western blotting**

105 　　　Following sedation with ketamine hydrochloride (10 mg/kg, i.m.) and xylazine

106 hydrochloride (1 mg/kg, i.m.), an intact monkey was anesthetized deeply with sodium

107 pentobarbital (50 mg/kg, i.v.) and perfused transcardially with 0.1 M

108 phosphate-buffered saline (PBS; pH 7.4). The MI (digit region) and the spinal cord (C7

109 to Th1 segments) were harvested and homogenized in a lysis buffer, comprising 50 mM

110 Tris-HCl (pH 7.8) with 150 mM NaCl, 1 mM EDTA, 2 mM $Na_3VO_4$, 1% NP-40, and

111 protease inhibitor cocktail. After centrifugation at 13,000 g for 20 min at 4˚C, it was

112 lysed by using equal amounts of 2 x sample buffer, comprising 250 mM Tris-HCl, 4%

113 sodium dodecyl sulphate, 20% glycerol, 0.02% bromophenol blue, and 5%

114 β-mercaptoethanol, and then proteins were boiled for 5 min at 95˚C. The mixed proteins

115 were separated on sodium dodecyl sulphate polyacrylamide gel electrophoresis and

116 transferred to a polyvinylidence fluoride membrane (Millipore). The membrane was

117 blocked with 5% skim milk in 0.01 M PBS containing 0.05% Tween-20 and then

118 incubated with anti-RGMa antibody (IBL). After several washes, the membrane was

119 incubated with horseradish peroxidase-linked anti-mouse IgG antibody (1:5,000; Cell

120 Signaling Technology). The detection was carried out with an ECL chemiluminescence

121 system (GE Healthcare). As control samples, human- and mouse-recombinant RGMa

122 proteins (R & D systems) were used.

123

124 **Experimental time-course**

125 The experimental time-course was summarized in Figure 1N. The monkeys

126 were trained with the two behavioral tasks, a reaching/grasping task and a modified

127 Brinkman board test (Freund et al., 2006, 2009) for 2–3 months prior to SCI. To reduce

128 the inter-animal variability in the modified Brinkman board test, pairs of monkeys who

129 exhibited similar baselines before SCI (i.e., Ctrl-A and RGMa-A, Ctrl-B and RGMa-B,

130 and Ctrol-C and RGMa-C) usually underwent simultaneous behavioral analyses. After

131 SCI, the two behavioral tasks were performed to assess the extent of recovered forelimb

132 movements over 14 weeks. Following all behavioral analyses, the digit regions of the

133 contralesional and ipsilesional MI were identified in the anti-RGMa antibody-treated

134 monkeys using intracortical microstimulation (ICMS), and then muscimol was injected

135 into the identified digit regions to inactivate neuronal activity therein. To examine

136    sprouting CST fibers below the lesioned site, biotinylated dextran amine (BDA) was

137    injected into the contralesional MI seven weeks prior to sacrifice. To label spinal

138    motoneurons through the median nerve on the SCI side, wheat germ

139    agglutinin-conjugated horseradish peroxidase (WGA-HRP) was infused from the cut

140    end of the nerve four days prior to sacrifice. One of the four monkeys (RGMa-B) who

141    were treated with the anti-RGMa antibody was excluded from the

142    electrophysiological/pharmacological and histological analyses, because this monkey

143    was dead by unknown accident shortly after the behavioral analyses.

144

145    **Behavioral analyses**

146        We investigated whether RGMa inhibition with the antibody might promote the

147    recovery from impaired manual dexterity after SCI. To assess the extent to which the

148    skilled motor behavior was restored in our SCI model, the two behavioral tasks, a

149    reaching/grasping task and a modified Brinkman board test were performed. These tasks

150    were designed to take out pellets from vertical and horizontal slots. Each behavioral

151    analysis was carried out on the 3rd, 5th, 7th, and 10th day after SCI, and then twice a

152    week until the 14th week.

153

154 <u>Reaching/grasping task</u>

155   This task was performed to assess quantitatively the extent of recovery of

156 dexterous manual movements as previously described (Nakagawa et al., 2015). Briefly,

157 the monkeys were seated in a primate chair, and an acrylic board which consisted of

158 three vertical or horizontal slots was placed in front of the chair (Fig. 4A,B). Each slot

159 was filled with a small pellet (diameter, 9 mm). The monkeys reached for the vertical or

160 horizontal slots and attempted to pick up three pellets within 10 sec in each trial. We

161 analyzed how many pellets the monkeys successfully collected in each session (7 trials).

162 Data were expressed as the ratio of the number of collected pellets to the total number

163 per session (21 pellets; 3 pellets x 7 trials) in each of the vertical-slot and horizontal-slot

164 tasks.

165

166 <u>Modified Brinkman board test</u>

167   The Brinkman board test was originally created to assess manual dexterity after

168 SCI at the cervical cord level in macaque monkeys (Rouiller et al., 1998). Later, Freund

169 et al. (2006, 2009) have made a minor modification for analyzing the extent of

170 functional recovery from SCI, and named it "a modified Brinkman board test". In the

171 present study, we applied this modified version. The monkeys were seated in a primate

172     chair, and the Brinkman board was placed on the chair. The Brinkman board (10 cm x

173     20 cm) was made of an acrylic board where a total of 50 slots (15 mm long x 8 mm

174     wide x 6 mm deep), consisting of 25 vertical and 25 horizontal slots, were randomly

175     located on the board (Fig. 4E). Each slot was filled with a food pellet (94 mg, banana or

176     very berry flavor; Bioserve). In our modified Brinkman board test, each session

177     consisted of 50 trials (25 trials for each of the vertical- and horizontal-slot tasks) to take

178     out a total of 50 pellets, and a trial was considered to be successful when the monkey

179     grasped a pellet and conveyed it to the mouth within 30 sec. On the other hand, a trial

180     was counted as an error when the monkey failed to grasp a pellet or dropped it on the

181     way to the mouth. The baseline value prior to SCI was represented as the mean of

182     successful trials (maximum = 25) per session in each of the vertical- and horizontal-slot

183     tasks that were performed 7 times (5 sessions per day). In each monkey, the analyzed

184     data were evaluated as the number of successful trials per session in a daily test.

185

186     **Surgical procedures for SCI**

187         Surgical procedures for SCI were performed as previously described with

188     minor modifications (Nakagawa et al., 2015). Briefly, the monkeys were sedated with a

189     combination of ketamine hydrochloride (10 mg/kg, i.m.), xylazine hydrochloride (1

190   mg/kg, i.m.), and atropine (0.05 mg/kg, i.m.), and then anesthetized with sodium

191   pentobarbital (25 mg/kg, i.v.). The monkeys who were monitored with percutaneous

192   oxygen saturation, respiration rate, heart rate, blood pressure, body temperature, and

193   electrocardiogram were stabilized in a stereotaxic frame. The skin and axial muscles

194   were dissected at the level of the C2 to T1 segments under aseptic conditions.

195   Subsequently, laminectomy of the C3 to C7 segments was performed, and the dura

196   mater was cut unilaterally. After identification of the dorsal roots at the C6 and C7

197   levels, a border between the C6 and the C7 segment was lesioned with a surgical blade

198   (No. 11) and a special needle (27G). The anti-RGMa antibody or control antibody (IgG

199   from mouse serum; Sigma-Aldrich) was continuously delivered, via an osmotic pump

200   (2ML4, Alzet) installed under the skin of the back, to the periphery of the lesioned site

201   over four weeks immediately after SCI. Both the anti-RGMa and the control antibodies

202   purified as IgGs were concentrated to 50 μg/kg/day in PBS. To estimate the extent of

203   antibody infusion in the spinal cord, a 1% solution of Fast blue (Polysciences) was used

204   instead of the antibody. To fix properly a catheter (11 cm long) attached to the osmotic

205   pump, the top of the catheter was placed 5 mm above the lesioned site under the dura

206   mater (intrathecal administration) following SCI, and the catheter was connected to the

207   dura mater and surrounding muscles with surgical suture to keep the position during the

208    delivery of the antibody (Fig. 1K). Subsequently, spongel (Astellas) was located on the

209    dura mater for hemostasis, and then the muscles and skin were sutured. Following the

210    surgery, the monkeys were given an analgesic (Lepetan; Otsuka; i.m.; Indomethacin;

211    Isei; oral, one week) and an antibiotic (Viccillin; Meiji Seika; i.m., 3–4 days). Four

212    weeks later, the osmotic pump was removed from the back under general anesthesia

213    (see above) and, then, checked to ensure that the whole amount of the antibody was

214    certainly delivered up.

215

216    **Intracortical microstimulation (ICMS)**

217    Under general anesthesia with sodium pentobarbital (25 mg/kg, i.v.), two pipes

218    made of polyether ether ketone were mounted in parallel over the frontal and occipital

219    lobes for head fixation. After partial removal of the skull over the central sulcus under

220    aseptic conditions, two rectangular plastic chambers (for the contralesional MI, 37 mm

221    long x 42 mm wide x 15 mm deep; for the ipsilesional MI, 28 mm long x 32 mm wide x

222    20 mm deep) were attached to the exposed skull. Several days later, each monkey was

223    seated in a primate chair with the head fixed in a stereotaxic frame attached to the chair.

224    A glass-coated tungsten microelectrode (0.5–1.5 MΩ at 1 kHz; Alpha Omega) was

225    penetrated perpendicularly into the contralesional or ipsilesional MI to identify the digit

226    region. Parameters of electrical stimulation were as follows: trains of 11 and 44 cathodal

227    pulses, 200-μsec duration at 333 Hz, current of less than 65 μA. Basically, movements

228    of the digits on the MI stimulation are easily elicited by short trains in a normal control

229    (Miyachi et al., 2005). However, as we could assume that the movement threshold for

230    ICMS might become higher after SCI, we used a 44-pulse train in addition to a 11-pulse

231    train. Evoked movements of the digits were carefully monitored by visual inspection

232    and muscle palpation.

233

234    **Muscimol injections**

235          To confirm whether compensatory pathways arising from the contralesional MI

236    might be involved in recovery from impaired manual dexterity in our SCI model, the

237    gamma-aminobutyric acid type A (GABA$_A$) receptor agonist, muscimol (1 μg/μl in

238    physiological      saline,      Sigma-Aldrich),      was      injected      into      the

239    electrophysiologically-identified digit region of the contralesional or ipsilesional MI

240    through a 10-μl Hamilton microsyringe following ICMS. At each of four loci, 3 μl of

241    muscimol was very slowly infused (Fig. 6A). Saline was injected into the same sites

242    using the same parameters as a control. After the muscimol or saline injections into the

243    MI digit region, skilled forelimb movements were assessed with the reaching/grasping

244 task (for horizontal slots). Data were expressed as the ratio of successfully collected

245 pellets to the total per session.

246

247 **Anterograde tract-tracing of CST fibers**

248    CST fibers below the lesioned site arising from the contralesional MI were

249 anterogradely labeled with biotinylated dextran amine (BDA; Invitrogen; 10,000 MW).

250 The BDA injections into the contralesional MI were performed seven weeks prior to

251 sacrifice as previously described (Nakagawa et al., 2015). Briefly, under general

252 anesthesia (see above), a 10% solution of BDA in PBS was extensively injected into

253 multiple loci along the central sulcus where regions representing not only the forelimb,

254 but also the trunk and hindlimb were located, through a 5-µl Hamilton microsyringe

255 (150 nl each penetration) (Fig. 1B).

256

257 **Motoneuron labeling through the median nerve**

258    To label spinal motoneurons through the median nerve on the SCI side, a 5%

259 solution of WGA-HRP in physiological saline (Sigma-Aldrich) was applied to the cut

260 end of the nerve four days prior to sacrifice. Under deep-anesthesia conditions (see

261 above), the skin and intermuscular septum of the arm were dissected, and the median

262 nerve was exposed. The nerve was fully transected approximately 3.5 cm distal to the

263 elbow joint. A total of 10 µl WGA-HRP was put inside a special tube, the cut end of the

264 nerve was immersed in the tracer solution for 10 min, and then, the muscles and skin

265 were sutured. Following the surgery, the monkeys were given the analgesic and

266 antibiotic.

267

268 **Histochemical and immunohistochemical procedures**

269 Following sedation with ketamine hydrochloride (10 mg/kg, i.m.) and xylazine

270 hydrochloride (1 mg/kg, i.m.), the monkeys were anesthetized deeply with sodium

271 pentobarbital (50 mg/kg, i.v.) and perfused transcardially with 10% formalin. The fixed

272 brain and spinal cord were removed, immersed in PBS containing 30% sucrose until

273 they sank, and then cut serially into 40-µm thick transverse sections (for the spinal cord)

274 or 50-µm thick frontal sections (for the brain) on a freezing microtome. Procedures for

275 histochemical visualization of injected and transported BDA with DAB-nickel and for

276 immunohistochemistry with the Vector NovaRed substrate kit (Vector laboratories) were

277 done as described elsewhere (Nakagawa et al., 2015). For immunofluorescence

278 histochemical procedures, floating sections were blocked with 2% normal goat or

279 donkey serum and 3% bovine serum albumin in PBS containing 0.1% Triton X-100 for

280    60 min. The sections were then incubated with primary antibodies for 120 min at room

281    temperature (RT), followed by two overnights at 4°C. Primary antibodies used in the

282    present study were as follows: mouse anti-RGMa (IBL), rabbit anti-Iba1 (Wako), goat

283    anti-ChAT (Millipore), mouse anti-NeuN (Millipore), goat anti-WGA (Vector

284    laboratories), rabbit anti-WGA (Sigma-Aldrich), guinea pig anti-VGluT1 (Millipore),

285    and sheep anti-Chx10 (Abcam) antibodies. The anti-WGA antibody was pre-absorbed

286    with powder of the monkey's brain and spinal cord for prevention of cross-reaction with

287    unknown endogenous molecules. The goat anti-WGA antibody was used for all analyses

288    except double immunostaining with the rabbit anti-WGA antibody in combination with

289    the goat anti-ChAT antibody. BDA immunofluorescence histochemistry was carried out

290    with Alexa Fluor 488-conjugated streptavidin two overnights at 4°C. Subsequently, the

291    sections were incubated with secondary antibodies for 120 min at RT in the dark.

292    Secondary antibodies used in this study were as follows: goat and donkey anti-mouse,

293    rabbit, goat, guinea pig, and sheep IgG Alexa Fluor 647, 568, and 488 (Invitrogen). To

294    reduce endogenous autofluorescence, the sections were immersed in a TrueBlack

295    (Biotium) solution diluted by 70% ethanol for 30 sec. All histochemical and

296    immunohistochemical images were acquired with a microscope (Biorevo BZ-9000,

297    Keyence) or a confocal laser-scanning microscope (Fluo View FV1000, Olympus and

298    LSM 800, Zeiss).

299

300    ***In situ* hybridization procedures**

301         Under deep anesthesia (see above), the monkeys underwent perfusion-fixation

302    with 4% paraformaldehyde (PFA) dissolved in 0.1 M phosphate buffer (PB; pH 7.4).

303    The brain was removed and immersed in a 30% sucrose solution containing 4% PFA at

304    4˚C overnight. *In situ* hybridization was performed as previously described with minor

305    modifications (Watakabe et al., 2007). Briefly, 40-µm-thick frontal sections were placed

306    onto glass slides (Thermo Fisher Scientific) and fixed with 4% PFA in PB for 15 min at

307    RT. The sections were treated sequentially with proteinase K (7.2 µg/ml) for 30 min at

308    37˚C, 4% PFA for 15 min at RT, 0.25% acetic anhydride in 0.1 M triethanolamine for 10

309    min at RT, 0.3% Triton X-100 in PB for 20 min at RT. Subsequently, the sections were

310    hybridized with a Digoxigenin (DIG)-labeled riboprobe (0.12 µg/ ml) for 16 hr at 68˚C

311    in a hybridization buffer comprising 50% formamide, 5x SSC, 5x Denhard's solution

312    (Invitrogen), 250 µg/ml tRNA (Roche Diagnostics), 500 µg/ml ssDNA (Sigma-Aldrich).

313    The riboprobe for *Neogenin* (XM_015142632.1; 346–979) was purchased from Geno

314    Staff (Tokyo, Japan) and heated at 80˚C for 5 min before use. After overnight, the

315    sections were washed with 0.2x SSC for 30 min x 3 at 68˚C. Next, the sections were

19

316    blocked with 1% blocking reagent (Roche Diagnostics) and 10% lamb serum in

317    Tris-buffered saline containing 0.05% Tween 20 (TBS) for 1 hr at RT and then

318    incubated with alkaline phosphatase-conjugated anti-DIG antibody (1:5,000 dilution,

319    Roche Diagnostics) in TBS containing 1% blocking reagent and 1% lamb serum for 2 hr

320    at RT. To visualize hybridization signals, the sections were immersed in a coloring

321    buffer containing nitroblue tetrazolium and 5-bromo-4-chloro-3-indolyl phosphate.

322

323    **Data analyses**

324    <u>Quantification of BDA-labeled CST fibers below the lesioned site</u>

325         BDA-labeled CST fibers in the C7, C8, and Th1 segments were quantified in

326    laminae VII and IX of transverse sections (400 μm apart) on the SCI side. Additionally,

327    BDA-labeled midline-crossing fibers from the ipsilateral and ventral CSTs were

328    quantified in each segment below the lesioned site. In lamina VII, the intensity of

329    BDA-labeled CST fibers stained by DAB reaction was measured within a rectangular

330    area (273 μm high x 362 μm wide) that was located 800 μm lateral to the center of the

331    central canal using an ImageJ software (National Institutes of Health, Bethesda, MD,

332    USA). Regarding lamina VII or IX, the number of contacts of BDA-labeled CST fibers

333    with single Chx10-labeled neuron (Immunofluorescence) or single WGA-HRP-labeled

20

334 motoneurons (DAB staining) was analyzed at a magnification of x400, respectively. The

335 contacts were defined by the presence of button-like swellings of BDA-labeled CST

336 fibers on somas or dendrites. The result was normalized by the mean number of

337 BDA-labeled CST fibers in the dorsolateral area at the C5 segment (three serial

338 sections) on the SCI side. BDA-labeled CST fibers that were observed in the gray

339 matter within a radius of 50 μm from the midline of the spinal cord on each of the SCI

340 and non-SCI sides were counted as midline-crossing fibers from the ipsilateral and

341 ventral CSTs (Fig. 5U). It should be noted here that such midline-crossing fibers may

342 contain some of contralaterally sprouting CST fibers. The result was normalized by the

343 mean number of BDA-labeled CST fibers in the dorsolateral area at each segment (three

344 serial sections) on the non-SCI side.

345

346 <u>Measurements of the extent of spinal cord lesions</u>

347 　　　　The extent of spinal cord lesions was measured, with the ImageJ software

348 described above, as the mean of the maximum lesioned area in three serial sections

349 which were Nissl-stained with 1% Cresyl violet (see also Nakagawa et al., 2015). The

350 lesioned area was expressed as the ratio to the total area of the hemi-transverse section

351 on the lesioned side.

352

**Statistics**

For behavioral analyses of the control antibody-treated and anti-RGMa antibody-treated monkey groups, two-way ANOVA was applied. Increases in BDA-labeled CST fibers in laminae VII, IX and the midline area (i.e., midline-crossing CST fibers) were analyzed by two-way ANOVA, followed by Student's $t$-test. For within-group comparisons for pre- versus post-muscimol injections in the reaching/grasping task and for the extent of spinal lesions, paired $t$-test was applied. All data were represented as mean ± S.E.M., and statistical significance was accepted at $P < 0.05$.

362

363 **Results**

364 **SCI model and the extent of spinal cord lesions**

365       In our SCI model, the spinal cord was unilaterally lesioned in macaque monkeys.

366 The lesions were made at the border between the C6 and the C7 level to infringe upon

367 the lateral area of the hemi-transverse section (Fig. 1A). When BDA was injected into

368 the contralateral (contralesional) MI, laterally-situated CST fibers were found to be fully

369 removed in all of the lesioned monkeys, and, therefore, no BDA-labeled CST fibers in

370 any cases were observed in the dorsolateral funiculus of the spinal cord below the

371 lesioned site (Figs. 1B-E,G-I and 2A; see also Fig. 5B,G,L). The lesioned sites in all SCI

372 monkeys were Nissl-stained to assess the ratio of the lesioned area, and there was no

373 marked difference between the control antibody-treated (control) monkey group and the

374 anti-RGMa antibody-treated (RGMa antibody-treated) monkey group (Fig. 2A,B). Part

375 of the medial gray matter was kept intact to retain a route of sprouting CST fibers in our

376 SCI model, and anterograde tract-tracing with BDA from the contralesional MI resulted

377 in CST fiber labeling in this area (Figs. 1C,D,F,H,J and 2A). To confirm cross-reaction

378 of the anti-RGMa antibody to the MI and the spinal cord of rhesus monkeys, western

379 blotting was performed. We observed double and triple bands in the monkey MI and

380 spinal cord (Fig. 1M). It has been reported that the RGMa protein is a tethered

23

381    membrane-bound molecule, and that proteolytic processing amplifies RGMa diversity

382    by creating soluble versions, the full-length and proteolytic cleavage RGMa, with

383    long-range effects (Tassew et al., 2009, 2012). The antibody was delivered continuously

384    to the lesioned site via the osmotic pump for four weeks immediately after SCI (Fig.

385    1K,L,N).

386

387    **Upregulation of RGMa around the lesioned site after SCI**

388        First, the expression patterns of RGMa and *Neogenin* (a receptor for RGMs)

389    were examined by immunohistochemistry or *in situ* hybridization in the cervical cord or

390    MI, respectively, in our SCI model (one intact and two lesioned monkeys; Fig. 3).

391    Longitudinal sections in the cervical cord ten days after SCI were immunostained with

392    the anti-RGMa antibody, and then the RGMa expression was compared with a region

393    remote from the lesioned site in the same section and with the same region in an intact

394    (uninjured) section (Fig. 3A–C,F). Our immnunohistochemical analyses revealed that

395    the RGMa expression was obviously increased around the lesioned site after SCI. Next,

396    we characterized RGMa-expressing cells by double immunofluorescence histochemistry

397    and found that RGMa was present in Iba1-positive cells (Fig. 3D–F). Thus, RGMa was

398    expressed in microglia/macrophages and upregulated specifically around the lesioned

24

399  site. In addition, *Neogenin* was expressed in layer 5 (identified in the adjacent

400  Nissl-stained sections) of the contralesional and ipsilesional MI (Fig. 3G–J).

401

402  **Effects of anti-RGMa antibody on impaired manual dexterity after SCI**

403      In the reaching/grasping task, the motor performance through both the

404  vertical-slot and the horizontal-slot tasks was greatly recovered in the RGMa

405  antibody-treated monkey group, compared with the control monkey group, to reach as

406  highly as the pre-SCI level (Fig. 4C,D, Video S1). Similar results were obtained in the

407  modified Brinkman board test, especially when the RGMa antibody-treated monkey

408  group took out pellets from vertical slots (Fig. 4F,G, Video S2). In the case where skilled

409  forelimb movements through the horizontal-slot task were attempted, the RGMa

410  antibody-treated monkey group did not so prominently exhibit functional recovery,

411  although motor behavior was improved in comparison with the control monkey group in

412  which no such movements were restored at all (Fig. 4H, Video S2). Moreover, our

413  behavioral analyses revealed that in both the reaching/grasping task and the modified

414  Brinkman board test, the antibody treatment against RGMa not only promoted the

415  recovery of motor functions, but also advanced the start of recovery following SCI (Fig.

416  4C,D,F–H).

417

**Increase in sprouting CST fibers with the neutralizing antibody against RGMa**

To begin with addressing the reorganization of CST fibers below the lesioned

site, we analyzed the distribution pattern of BDA-labeled CST fibers in the C7, C8, and

Th1 segments. We observed no BDA-labeled CST fibers in the dorsolateral funiculus in

both the control and the RGMa antibody-treated monkey groups (Fig. 5A,B,F,G,K,L).

Approximately 30–50% of the BDA-labeled CST fibers, relative to an intact monkey,

was found in lamina VII of the RGMa antibody-treated monkey group, whereas less

than 10% of them were seen in lamina VII of the control monkey group (Fig.

5A,C,F,H,K,M,P). In lamina IX, all WGA-HRP-labeled neurons corresponded with

ChAT-positive motoneurons (Fig. 5D'), indicating that all of them are motoneurons for

the median nerve. In the RGMa antibody-treated monkey group, the number of contacts

of sprouting CST fibers with single WGA-positive neurons was increased in lamina IX

below the lesioned site, compared with the control monkey group (Fig.

5A,D,E,F,I,J,K,N,O,Q,E'). At least part of the sprouting CST fibers seemed to be in

contact with spinal interneurons immunolabeled for Chx10. Similarly, we observed that

the sprouting CST fibers in the RGMa antibody-treated monkey group appeared to make

contact with single Chx10-positive neurons more frequently than in the control monkey

26

435     group (Fig. 5W-B',C'). We found a certain difference in the reinnervation pattern of

436     sprouting CST fibers in each segment. In lamina VII, the intensity of BDA-labeled CST

437     fibers and the number of contacts of these CST fibers with single Chx10-positive

438     neurons were gradually decreased as the distance from the lesioned site became larger

439     (C7 < C8 < Th1) in the RGMa antibody-treated monkey group. By contrast, the number

440     of contacts of sprouting CST fibers with single WGA-positive neurons was increased in

441     the same group, which was similar to the findings in an intact monkey (Fig. 5P,Q,C').

442     The number of midline-crossing fibers was also increased by the neutralizing antibody

443     against RGMa (Fig. 5R–V). It should be noted here that the midline-crossing fibers

444     observed may involve some extended fibers from the injured CST.

445

446     **Impairments in recovered manual dexterity by muscimol inactivation in the**

447     **contralesional MI**

448         Following all behavioral analyses, ICMS was performed in the contralesional

449     and ipsilesional MI of both the control and the RGMa antibody-treated monkey groups

450     whether the contralesional MI might contribute to the functional recovery from impaired

451     manual dexterity due to SCI (Fig. 1N). The movements of the digits ipsilateral to SCI

452     were successfully elicited by intracortical microstimulation in four loci of the

27

453    contralesional MI, but not of the ipsilesional MI in the RGMa antibody-treated SCI

454    monkeys (Fig. 6A). Subsequent injections of muscimol into all of the

455    electrophysiologically-identified digit region of the contralesional MI, but not of the

456    ipsilesional MI, induced reversible impairments in skilled forelimb movements on the

457    SCI side (Fig. 6C,D). The reaching/grasping task (for horizontal slots) was employed to

458    assess the motor function. About 20 min after the muscimol injections, manual dexterity

459    was gradually deteriorated and severely impaired within one hour. Thereafter, impaired

460    forelimb movements were continually seen for a few hours. Although all RGMa

461    antibody-treated monkeys could move the digits individually on the next day, manual

462    dexterity was not so sufficiently restored, as compared to that before the muscimol

463    injections into the contralesional MI. When we carried out the ICMS experiment in the

464    control monkey group, no movements of the digits were evoked in the contralesional MI

465    (Fig. 6B). In general, the digit region of the MI was surrounded by the regions

466    representing the wrist, elbow, and face in macaque monkeys (Sessle and Wiesendanger,

467    1982). However, a sector surrounded by the wrist, elbow, and face regions exhibited no

468    response to ICMS (Fig. 6B). As we could not identify the digit region in the

469    contralesional MI of the control monkey group, we injected muscimol only into the

470    ipsilesional MI. Then, the muscimol injections into the digit region of the ipsilesional MI

471    induced reversible impairments in skilled movements of the SCI-unimpaired forelimb

472    only on the uninjured side (Fig. 6E), just like the RGMa antibody-treated monkey group

473    (Fig. 6D).

474

**Discussion**

475

476    Owing to the low capacity of growth/regeneration in the mature CNS, various

477    therapeutic approaches to CNS injures have been attempted against extrinsic and intrinsic

478    inhibiting factors using *in vivo* and *in vitro* experiments with rodents (Sandvig et al.,

479    2004; Hata et al., 2006; Mar et al., 2014). According to previous works (Yiu and He,

480    2006; Popovich and Longbrake, 2008; Rolls et al., 2009) glial cells expressing

481    growth-inhibiting factors are rich in the lesioned area after SCI in rodents, and immune

482    and inflammatory cells are also accumulated in the same area. It has repeatedly been

483    demonstrated that RGMa is expressed in these cells (Schwab et al., 2005; Mirakaj et al.,

484    2010; Muramatsu et al., 2011). The present study revealed that RGMa was specifically

485    upregulated around the lesioned site with increases in microglia/macrophages after SCI

486    (see Fig. 3D,E).

487    The spinal cord repair strategies through growing/regenerating axons include a

488    series of events, consisting of the initiation of axonal growth, the maintenance of axonal

489    elongation, the connectivity with appropriate target neurons, and the reorganization of

490    neural circuitry (Bradbury and McMahon, 2006). In rodent SCI models, a

491    reaching/grasping behavior was promoted by enhanced sprouting CST fibers, and many

492    of these fibers were extended through the medial part of the spinal cord (Hollis et al.,

493    2016). Thus, the enhanced sprouting CST fibers would make a synaptic connection with

494    spinal interneurons as the target for restoration of forelimb functions in rodents. For a

495    precision grip in higher primates, corticomotoneuronal pathway neurons in the MI are

496    specifically activated (Muir and Lemon, 1983). Moreover, during the monkey's

497    performance of a pinching task, motor commands descending to spinal motoneurons are

498    mediated at least partly by the spinal interneurons (Takei and Seki, 2010, 2013). Taken

499    together, it is most likely that the reorganization of both the direct and the indirect (via

500    the spinal interneurons) corticomotoneuronal pathways is required to promote recovery

501    from impaired manual dexterity through enhanced sprouting of CST fibers in our SCI

502    model.

503        In our behavioral tasks, to take out pellets skillfully from vertical and horizontal

504    slots, cortically-derived compensatory input would be transmitted to the motoneurons

505    and/or interneurons in the C7, C8, and Th1 segments that are situated below the SCI site.

506    Particularly when taking out a pellet from the horizontal slot in the modified Brinkman

507    board test, the monkey is required to move the wrist to the ulnar direction for achieving

508    digit flexion with ulnar deviation. It has been reported that the wrist angle in the ulnar

509    direction is largely reduced after SCI when the monkey takes out a pellet from the

510    horizontal slot (Hoogewoud et al., 2013). In macaque monkeys, spinal motoneurons

511  innervating the extensor carpi ulnaris muscle responsible for digit flexion with ulnar

512  deviation are mainly distributed in the C8 and Th1 segments (Jenny and Inukai, 1983;

513  Schieber, 1995).

514     We demonstrated that sprouting CST fibers originating from the contralesional

515  MI in RGMa antibody-treated monkeys penetrated more densely, compared with the

516  control monkey group, into laminae VII and IX where spinal interneurons and

517  motoneurons were located, respectively, below the lesioned site (see Fig. 5P,Q). In our

518  experiments, the motoneurons in the C7, C8, and Th1 segments were labeled through

519  the median nerve that predominantly governs the distal forelimb muscles, activity of

520  which is essential for execution of manual dexterity with a precision grip (Dun et al.,

521  2007). In addition, a large number of motoneurons for hand (digits) muscles in primates

522  are located in the Th1 segment (Jenny and Inukai, 1983). With respect to the pattern of

523  reinnervation of the enhanced corticomotoneuronal pathway after SCI with the

524  anti-RGMa antibody treatment, sprouting CST fibers might lead to appropriate target

525  motoneurons with guidance factors to promote the recovery of motor functions

526  effectively and efficiently.

527     At least part of sprouting CST fibers seemed to be in contact with the

528  interneurons immunolabeled for Chx10. Chx10 was originally identified as one of the

529　markers for glutamatergic interneurons in rodents (Ericson et al., 1997), and

530　Chx10-positive neurons are reportedly distributed throughout the hindbrain and the

531　spinal cord in mammals and regulate motor functions, such as breathing and locomotion

532　(Ai-Mosawie et al., 2007; Crone et al., 2008, 2012; Dougherty and Kiehn, 2010; Azim

533　et al., 2014). According to a recent work (Liu et al., 2015), there is a correlation between

534　the number of Chx10-positive neurons in contact with sprouting CST fibers and

535　functional recovery of the forelimb with unilateral cervical cord injury in mice. Together

536　with the direct corticomotoneuronal pathway, the compensatory indirect pathway via

537　spinal interneurons may also be crucial to the recovery of a series of forelimb

538　movements, reaching for slots and taking out pellets from slots using a precision grip, in

539　our SCI model.

540　　　Interestingly, according to our behavioral analyses, the antibody treatment

541　against RGMa not only promoted the recovery of motor functions, i.e., the ability to

542　move the digits individually, but also advanced the start of recovery following SCI. It

543　has been well documented that treatment with the RGMa-neutralizing antibody in a

544　rodent model of multiple sclerosis promotes functional recovery by preventing

545　neurodegeneration (Muramatsu et al., 2011; Tanabe and Yamashita, 2014; Demicheva et

546　al., 2015). Recently, it has been reported that the RGMa antibody treatment promoted

547 neuronal survival around the lesioned site with improvement of functional recovery in a

548 rodent SCI model (Mothe et al., 2017). Moreover, RGMa has been shown to reduce

549 leukocyte trafficking and retard inflammation (Mirakaj et al., 2010). Thus, RGMa

550 suppression has a certain impact on neuroprotection as well as on neurite outgrowth,

551 and, therefore, the present results might be ascribed, at least partly, to the

552 neuroprotective effect of the RGMa antibody.

553     The spinal cord lesions in some cases (i.e., Ctrl-B and RGMa-A monkeys)

554 infringed, to some extent, upon uncrossed ventral CST region, though it almost

555 unaffected recovery of manual dexterity, especially in the RGMa antibody-treated

556 (RGMa-A) monkey (data not shown). It has previously been reported that the ventral

557 CST distributes the fibers to proximal muscles, such as the neck, trunk, and proximal

558 upper extremities (Nyberg-Hansen, 1963; Davidoff, 1990; Canedo, 1997). The motor

559 tasks that we used in the present work (i.e., reaching/grasping task and the modified

560 Brinkman board test) are required for movements of the proximal upper limb, but the

561 spinal region responsible for the proximal upper limb remains intact in our SCI model.

562     By carrying out a series of pharmacological experiments following ICMS, we

563 have demonstrated that the contralesional MI is greatly involved in recovery from

564 impaired manual dexterity in our SCI model with the anti-RGMa antibody treatment. In

34

565 the control monkey group, on the other hand, forelimb movements once impaired by

566 SCI could not be evoked at all by our ICMS protocol (44-pulse train, 65-µA current).

567 This may depend on an increase in sprouting CST fibers from the contralesional MI to

568 the cervical cord on the injured side. Additionally, it should be noted here that other

569 descending pathways, including the cortico-brainstem and cortico-propriospinal

570 pathways, might contribute to the functional recovery (Isa et al., 2013). In a similar

571 primate model of SCI (C7/C8 lesion model), reorganization of CST fibers originating

572 from the contralesional MI with the somatotopic map altered is crucial to recovery of

573 motor functions (Schmidlin et al., 2004, 2005). Part of uncrossed CST fibers derived

574 from the ipsilesional MI was disrupted in our SCI model, and, also, *Neogenin* was

575 expressed in layer 5 of the ipsilesional MI as well as of the contralesional MI (see Fig.

576 3I,J). RGMa has been shown to evoke the strong inhibition of axonal outgrowth and

577 regrowth through the transmembrane receptor, Neogenin (Tassew et al., 2014). Hence, it

578 can be considered that injured CST fibers extend beyond the lesioned site from the

579 ipsilesional MI by the aid of the anti-RGMa antibody. However, the CST fibers arising

580 from the ipsilesional MI may not work as a functional wiring at a late stage after SCI. In

581 view of the fact that the ipsilesional MI is activated at an early, but not a late stage of

582 recovery in a different primate model of SCI (Nishimura et al., 2007), the ipsilesional

583     MI might participate in functional restoration only transiently.

584          The present study defines that RGMa is a critical target molecule to promote

585     recovery from impaired manual dexterity after SCI. The antibody treatment against

586     RGMa may probably be applied not only to SCI, but also to other CNS insults, such as

587     traumatic brain injuries, stroke, and multiple sclerosis.

588

600

601 **References**

602 AI-Mosawie A, Wilson JM, Brownstone RM. 2007. Heterogeneity of V2-derived

603     interneurons in the adult mouse spinal cord. Eur J Neurosci. 26:3003–3015.

604 Azim E, Jiang J, Alstermark, B, Jessell TM. 2014. Skilled reaching relies a V2a

605     propriospinal internal copy circuit. Nature. 508:357–363.

606 Bradbury EJ, McMahon SB. 2006. Spinal cord repair strategies: why do they work? Nat

607     Rev Neurosci. 7:644–653.

608 Canedo A. 1997. Primary motor cortex influences on the descending and ascending

609     systems. Prog Neurobiol. 51:287–335.

610 Crone SA, Quinlan KA, Zagoraiou L, Droho S, Restrepo CE, Lundfald L, Endo T,

611     Setlak J, Jessell TM, Kiehn O, et al. 2008. Genetic ablation of V2a ipsilateral

612     interneurons disrupts left-right locomotor coordination in mammalian spinal cord.

613     Neuron. 60:70–83.

614 Crone SA, Viemari JC, Droho S, Mrejeru A, Ramirez JM, Sharma K. 2012. Irregular

615     breathing in mice following geneticablation of V2a neurons. J Neurosci.

616     32:7895–7906.

617 Davidoff RA. 1990. The pyramidal tract. Neurology. 40:332-339.

618    Demicheva E., Cui YF, Bardwell P, Barghom S, Kron M, Meyer AH, Schmidt M,

619    Gerlach B, Leddy M, Barlow E, et al. 2015. Targeting repulsive guidance molecule

620    A to promote regeneration and neuroprotection in multiple sclerosis. Cell Rep.

621    10:1887–1898.

622    Dougherty KJ, Kiehn O. 2010. Functional organization of V2a-related locomotor

623    circuits in the rodent spinal cord. Ann. NY Acad Sci. 1198:85–93.

624    Dun S, Kaufmann RA, Li ZM. 2007. Lower median nerve block impairs precision grip.

625    J Electromyogr Kinesiol. 17:348–354.

626    Ericson J, Rashbass P, Schedl A, Brenner-Morton S, Kawakami A, van Heyningen V,

627    Jessell TM, Briscoe J. 1997. Pax6 controls progenitor cell identify and neuronal

628    fate in response to graded Shh signaling. Cell. 90:1169–180.

629    Freund P, Schmidlin E, Wannier T, Bloch J, Mir A, Schwab ME, Rouiller, EN. 2006.

630    Nogo-A–antibody treatment enhances sprouting and functional recovery after

631    cervical lesion in adult primates. Nat Med. 12:790–792.

632    Freund P, Schmidlin E, Wannier T, Bloch J, Mir A, Schwab ME, Rouiller EN. 2009.

633    Anti-Nogo–A antibody treatment promotes recovery of manual dexterity after

634    unilateral cervical lesion in adult primates – re-examination and extension of

635    behavioral data. Eur J Neurosci. 29:983–996.

636     GrandPré T, Li S, Strittmatter SM. 2002. Nogo-66 receptor antagonist peptide promotes

637         axonal regeneration. Nature. 417:547–551.

638     Hata K, Fujitani M, Yasuda Y, Doya H, Saito T, Yamagishi S, Mueller BK, Yamashita

639         T. 2006. RGMa inhibition promotes axonal growth and recovery after spinal cord

640         injury. J Cell Biol. 173:47–58.

641     Hollis ER 2nd, Ishiko N, Yu T, Lu CC, Haimovich A, Tolentino K, Richman A, Tury A,

642         Wang SH, Pessian M, et al. 2016. Ryk controls remapping of motor cortex during

643         fanctional recovery after spinal cord injury. Nat Neurosci. 19:697–705.

644     Hoogewoud F, Hamadjida A. Wyss AF, Mir A, Schwab ME, Belhaj-Saif A, Rouiller

645         EM. 2013. Comparison of functional recovery of manual dexterity after unilateral

646         spinal cord lesion or motor cortex lesion in adult macaque monkeys. Front Neurol.

647         4:101.

648     Isa T, Kinoshita M, Nishimura Y. 2013. Role of direct vs. indirect pathways from the

649         motor cortex to spinal motoneurons in the control of hand dexterity. Front Neurol.

650         4:191.

651     Jenny AB, Inukai J. 1983. Principles of motor organization of the monkey cervical

652         spinal cord. J Neurosci. 3:567–575.

653 Lah GL, Key B. 2012. Dual roles of the chemorepellent axon guidance molecule RGMa

654     in establishing pioneering axon tracts and neural fate decisions in embryonic

655     vertebrate forebrain. Dev Neurobiol. 72:1458–1470.

656 Lemon RN. 1993. The G. L. Brown Prize Lecture. Cortical control of the primate hand.

657     Exp Physiol. 78:263–301.

658 Liu ZH, Yip PK, Adams L, Davies M, Lee JW, Michael GJ, Priestley JV, Michael-Titus

659     AT. 2015. A single bolus of docosahexaenoic acid promotes neuroplastic changes

660     in the innervation of spinal cord interneurons and motor neurons and improves

661     functional recovery after spinal cord injury. J Neurosci. 35:12733–12752.

662 Mar FM, Bonni A, Sousa MM. 2014. Cell intrinsic control of axon regeneration. EMBO

663     Rep. 15:254–263.

664 Matsunaga E, Nakamura H, Chedotal A. 2006. Repulusive guidance molecule plays

665     multipleroles in neuronal differentiation and axon guidance. J Neurosci.

666     26:6082–6088.

667 Matsunaga E, Tauszing-Delamasure S, Monnier PP, Mueller BK, Strittmatter SM,

668     Mehlen PCHedotal A. 2004. RGM and its receptor neogenin regulate neuronal

669     survival. Nat Cell Biol. 6:749–755.

670    Mirakaj V, Brown S, Laucher S, Steinl C, Klein G, Köhler D, Skutella T, Meisel C,

671        Brommer B, Rosenberger P, et al. 2010. Repulsive guidance molecule-A (RGM-A)

672        inhibits leukocyte migration and mitigates inflammation. Proc Natl Acad Sci USA.

673        108:6555–6560.

674    Miyachi S, Lu X, Inoue S, Iwasaki T, Koike S, Nambu A, Takada M. 2005.

675        Organization of multisynaptic inputs from prefrontal cortex to primary motor cortex

676        as revealed by retrograde transneuronal transport of rabies virus. J Neurosci.

677        25:2547–2556.

678    Monnier PP, Sierra A, Macchi P, Deitinghoff L, Andersen JS, Mann M, Flad M,

679        Homberger MR, Stahl B, Bonhoeffer F, Mueller BK. 2002. RGM is a repulsive

680        guidance molecule for retinal axons. Nature. 419:392–395.

681    Mothe AJ, Tassew NG, Shabanzadeh AP, Penheiro R, Vigouroux RJ, Huang L,

682        Grinnell C, Cui YF, Fung E, Monnier PP, et al. 2017. RGMa inhibition with human

683        monoclonal antibodies promotes regeneration, plasticity and repair, and attenuates

684        neuropathic pain after spinal cord injury. Sci Rep. 7:10529.

685    Muir RB, Lemon RN. 1983. Corticospinal neurons with a special role in precision grip.

686        Brain Res. 261:312–316.

687    Muramatsu R, Kubo T, Mori M, Nakamura Y, Fujita Y, Akutsu T, Okuno T, Taniguchi

688        J, Kumanogoh A, Yoshida M, et al. 2011. RGMa modulates T cell responses and is

689        involved in autoimmune encephalomyelitis. Nat Med. 17:488–494.

690    Nakagawa H, Ninomiya T, Yamashita T, Takada M. 2015. Reorganization of

691        corticospinal tract after spinal cord injury in adult macaques. Sci Rep. 5:11986.

692    Nishimura Y, Onoe H, Morichika Y, Perfiliev S, Tsukada H, Isa T. 2007.

693        Time-dependent central compensatory mechanisms of finger dexterity after spinal

694        cord injury. Science. 318:1150–1155.

695    Nyberg-Hansen R. 1963. Some comments on the pyramidal tract, with special reference

696        to its individual variations in man. Acta Neurol Scand. 39:1–30.

697    Oudega M, Perez MA. 2012. Corticospinal reorganization after spinal cord injury. J

698        Physiol. 590:3647–3663.

699    Popovich PG, Longbrake EE. 2008. Can the immune system be harnessed to repair the

700        CNS? Nat Rev Neurosci. 9:481–493.

701    Rolls A, Shechter R, Schwartz M. 2009. The bright side of the glial scar in CNS repair.

702        Nat Rev Neurosci. 10:235–241.

703    Rouiller EM, Yu XH, Moret V, Tempini A, Wiesendanger M, Liang E, 1998. Dexterity

704        in adult monkeys following early lesion of the motor cortical hand area: the role of

705        cortex adjacent to the lesion. Eur J Neurosci. 10:729–740.

706    Sandvig A, Berry M, Butt A, Longan A. 2004. Myelin-, reactive glia-, and scar-derived

707        CNS axon growth inhibitors: expression, receptor signaling, and correlation with

708        axon regeneration. Glia. 46:225–251.

709    Schieber MH. 1995. Muscular production of individuated finger movements: the roles

710        of extrinsic finger muscles. J Neurosci. 15:284–297.

711    Schmidlin E, Wannier T, Bioch J, Ruiller EM. 2004. Progressive plastic change in the

712        hand representation of the primary motor cortex parallel incomplete recovery from

713        a unilateral section of the corticospinal tract at cervical level in monkeys. Brain Res.

714        1017:172–183.

715    Schmidlin E, Wannier T, Bioch J, Belhaj-Saif A, Wyss AF, Ruiller EM. 2005.

716        Reduction of the hand representation in the ipsilateral primary motor cortex

717        following unilateral section on the corticospinal tract at cervical level in monkeys.

718        BMC Neurosci. 6:56.

719 Schwab JM, Conrad S, Monnier PP, Julien S. Mueller BK, Schluesener HJ. 2005.

720 Spinal cord injury-induced lesional expression of the repulsive guidance molecule

721 (RGM). Eur J Neurosci. 21:1569–1576.

722 Sessle BJ, Wiesendanger M. 1982. Structural and functional definition of the motor

723 cortex in the monkey (*Macaca fascicularis*). J Physiol. 323:245–265.

724 Stahl B, Muller B, von Boxberg Y, Cox, EC, Bonhoeffer F. 1990. Biochemical

725 characterization of a putative axonal guidance molecule of the chick visual system.

726 Neuron. 5:735–743.

727 Takei T, Seki K. 2010. Spinal interneurons facilitate coactivation of hand muscles

728 during a precision grip task in monkeys. J Neurosci. 30:17041–17050.

729 Takei T, Seki K. 2013. Spinal premotor interneurons mediate dynamic and static motor

730 commands for precision grip in monkeys. J Neurosci. 33:8850–8860.

731 Tanabe S, Yamashita T. 2014. Repulusive guidance molecule-a is involved in

732 Th17-cell-induced neurodegeneration in autoimmune encephalomyelitis. Cell Rep.

733 9:1459–1470.

734 Tassew NG, Charish J, Chestopalova L, Monnier PP. 2009. Sustained *in vivo* inhibition

735 of protein domains using single-chain Fv recombinant antibodies and its application

736 to dissect RGMa activity on axonal outgrowth. J Neurosci. 29:1126–1131.

737    Tassew NG, Charish J, Seidah NG, Monnier PP. 2012. SKI-1 and Furin generate

738        multiple RGMa fragments that regulate axonal growth. Dev Cell. 22:391‑402.

739    Tassew NG, Mothe AJ, Shabanzadeh AP, Banerjee P, Koeberle PD, Bremner R, Tator

740        CH, Monnier PP. 2014. Modifying lipid rafts promotes regeneration and functional

741        recovery. Cell Rep. 8:11146–1159.

742    Vavrek R, Girgis J, Tetzlaff W, Hiebert GW, Fouad K. 2006. BDNF promotes

743        connections of corticospinal neurons onto spared descending interneurons in spinal

744        cord injured rat. Brain. 129:1534–1545.

745    Wahl AS, Omlor W, Rubio JC, Chen JL, Zheng H, Schröter A, Gullo M, Weinmann O,

746        Kobayashi K, Helmchen F, et al. 2014. Neuronal repair. Asynchronous therapy

747        restores motor control by rewiring of the rat corticospinal tract after stroke. Science.

748        34:1250–1255.

749    Watakabe A, Ichinohe N, Ohsawa S, Hashikawa T. Komatsu Y, Rockland KS,

750        Yamamori T. 2007. Comparative analysis of layer-specific genes in Mammalian

751        neocortex. Cereb Cortex. 17:1918–1933.

752    Yiu G, He Z. 2006. Glial inhibition of CNS axon regeneration. Nat Rev Neurosci.

753        7:617–627.

754

**Figure legends**

756 **Figure 1. SCI model and experimental time-course.**

757 (A) Schematic diagram showing our primate model of SCI. Unilateral lesions were made

758 at a border between the C6 and the C7 segment. Asterisk indicates the lesioned site. (B)

759 Example of the injection site in the contralesional MI. (C and G) Nissl-stained transverse

760 sections in the injured (SCI) and uninjured spinal cords. The strongly stained area

761 represents the lesion extent in panel C. (D and H) Transverse sections labeled with BDA

762 injected into the contralesional or contralateral MI in the injured or uninjured spinal cord,

763 respectively. The dotted line demarcates the lesioned area in panel D. (E and I)

764 Higher-power magnifications of areas in the dorsolateral funiculus in panels D and H,

765 respectively. (F and J) Higher-power magnifications of areas in the medial gray matter in

766 panels D and H, respectively. Note that BDA-labeled CST fibers extend beyond the

767 lesioned site through the intact medial gray matter in the injured spinal cord. (K)

768 Schematic diagram showing the antibody delivery system using an osmotic pump. (L)

769 Anti-RGMa antibody delivered around the lesioned site via an osmotic pump. To

770 visualize the extent of antibody infusion, Fast blue was used. (M) Western blot analysis of

771 the anti-RGMa antibody. The antibody crosses to the MI and the spinal cord of a rhesus

772    monkey. (N) Experimental time-course. Scale bars, B and C 1 mm for B to D and G, H,

773    for B, C, E; J 50 μm for E, F, I and J.

774

775    **Figure 2. Extent of spinal cord lesions.**

776    (A) Extent of SCI (in blue) in a representative transverse section in each monkey. (B)

777    Ratio of the lesioned area to the total area in a hemisection in each of control

778    antibody-treated (Ctrl) and anti-RGMa antibody-treated (RGMa) monkeys. There is no

779    marked difference in the averaged ratio between the two monkey groups. Because of the

780    death by unknown accident shortly after the behavioral analyses, monkey RGMa-B was

781    excluded from the electrophysiological/pharmacological and histological analyses.

782

783    **Figure 3. Expression patterns of RGMa and *Neogenin* in the cervical cord and MI.**

784    (A) RGMa expression (in purple) around the lesioned site (at the C6/C7 border) 10 days

785    after SCI in a longitudinal section. Shown in black are CST fibers anterogradely labeled

786    after BDA injections into the contralesional MI. (B) RGMa expression in a region

787    remote from the lesioned site in the same section. (C) RGMa expression in the same

788    region as in panel A in a normal (uninjured) case. (D and E) Expression of RGMa in

789    combination with Iba1 around the lesioned site. (F) Schematic diagram representing the

48

790 approximate locations of panels A, B, D, and E. (G) *In situ* hybridization for *Neogenin*

791 messenger RNA in layer 5 (V) of the contralesional MI 10 days after SCI in a frontal

792 section. (H) Higher-power magnification of a square area in panel G. (I) *In situ*

793 hybridization for *Neogenin* messenger RNA in layer 5 (V) of the ipsilesional MI 10

794 days after SCI in a frontal section. (J) Higher-power magnification of a square area in

795 panel I. Scale bars, A, 50 μm for A to C; D,G,I, 200 μm; E,H,J, 50 μm.

796

797 **Figure 4. Recovery from impaired manual dexterity with the neutralizing antibody**

798 **against RGMa.**

799 (A and B) Reaching/grasping task. The monkey reaches for vertical (A) or horizontal (B)

800 slots and grasps pellets. (C and D) Ratio of pellets collected through vertical (C) or

801 horizontal (D) slots. (E) Modified Brinkman board test. The monkey takes out pellets

802 from randomly-set vertical and horizontal slots. (F) Total number of pellets collected

803 through vertical and horizontal slots. (G and H) Number of pellets collected through

804 vertical (G) or horizontal (H) slots. All data are based on three control antibody-treated

805 (Ctrl) and four anti-RGMa antibody-treated (RGMa) monkeys. Error bars denote S.E.M.

806 (two-way ANOVA, *$P < 0.05$).

807

808 **Figure 5. Sprouting of CST fibers with the neutralizing antibody against RGMa.**

809 (A, F, and K) BDA-labeled CST fibers in the Th1 segment in an intact (Uninjured; A), a

810 control antibody-treated (Ctrl; F) and an anti-RGMa antibody-treated (RGMa; K)

811 monkey. (B, G, and L) Higher-power magnifications of areas of the dorsolateral

812 funiculus in panels A, F, and K, respectively. (C, H, M, D, I, and N) Higher-power

813 magnifications of areas of laminae VII (C, H, and M) and IX (D, I, and N) in panels A, F,

814 and K, respectively. (E, J, and O) Higher-power magnifications of dotted zones in panels

815 D, I, and N, respectively. (P) Intensity of BDA-labeled CST fibers in lamina VII in the

816 intact (Uninjured; $n = 1$), control antibody-treated (Ctrl; $n = 3$), and anti-RGMa

817 antibody-treated (RGMa; $n = 3$) monkey groups. (Q) Number of contacts of BDA-labeled

818 CST fibers with single WGA-positive motoneurons in lamina IX in the same monkey

819 groups as in panel P. (R, S, and T) BDA-labeled CST fibers crossing the midline of the

820 spinal cord in an intact (Uninjured; R), a control antibody-treated (Ctrl; S), and an

821 anti-RGMa antibody-treated (RGMa; T) monkey. BDA was injected into the

822 contralateral or contralesional MI. (U) Schematic diagram showing the midline area

823 examined. CC, central canal. (V) Number of midline-crossing CST fibers below the

824 lesioned site (i.e., C7, C8, and Th1 segments). (W, Y, and A') Spinal interneurons

825 triple-labeled for BDA, NeuN, and Chx10 in lamina VII of the Th1 segment in an intact

826    (Uninjured; W), a control antibody-treated (Ctrl; Y), and an anti-RGMa antibody-treated

827    (RGMa; A') monkey. (X, Z, and B') Higher-power magnifications of dotted zones in

828    panels W, Y, and A', respectively. BDA-labeled CST fibers in contact with single

829    Chx10-positive neurons (specified by arrowheads). (C') Number of contacts of

830    BDA-labeled CST fibers with single Chx10-positive neurons in lamina VII in the same

831    monkey groups as in panels P and Q. (D') Motoneurons double-labeled for WGA-HRP

832    through the median nerve and ChAT in lamina IX of the Th1 segment in an anti-RGMa

833    antibody-treated monkey. All WGA-HRP-labeled neurons are ChAT-positive. The

834    dotted line indicates the border between the gray and the white matter. (E') Triple

835    labeling for BDA, WGA-HRP, and VGluT1 in lamina IX of the Th1 segment in an

836    anti-RGMa antibody-treated monkey. A BDA-labeled CST fiber in contact with a single

837    WGA-positive motoneuron (specified by arrowheads). Scale bars, A, 1 mm for A,F,K; N,

838    100 μm for B to D, G to I, L to N; O, 50 μm for E, J and O; R, 100 μm for R, S and T; W,

839    200 μm for W, Y and A'; X and D', 5 μm for X, Z, B' and D'; C', 200 μm. Error bars

840    denote S.E.M. (two-way ANOVA, followed by Student's *t*-test, *$P < 0.05$).

841

842    **Figure 6. Effects of muscimol injections into the MI on manual dexterity.**

843  (A) Sites of muscimol injections into the contralesional and ipsilesional MI in a

844  representative anti-RGMa antibody-treated monkey (RGMa-A). Filled circles indicate

845  the injection loci in all of which ICMS induced movements of the digits on the

846  contralateral side. AS, arcuate sulcus; CS, central sulcus. Scale bar, 2 mm. (B) Results of

847  ICMS mapping of the contralesional MI in a representative control antibody-treated

848  monkey (Ctrl-C). Each letter denotes the electrophysiologically-identified body part as

849  follows: E, elbow; F, face; W, wrist; X, no response. Scale bar, 2 mm. (C–E) Skilled

850  movements after muscimol injections into the digit region of the contralesional MI (C) or

851  the ipsilesional MI (D) in the anti-RGMa antibody-treated monkey group ($n = 3$), or of the

852  contralesional MI in the control antibody-treated monkey group (E; $n = 3$). Manual

853  dexterity that had been impaired by SCI and then recovered by RGMa treatment

854  (SCI-impaired forelimb) was again impaired after muscimol (but not saline) injections

855  into the contralesional MI. On the other hand, the muscimol injections into the

856  ipsilesional MI only caused impairments in skilled movements of the normal forelimb

857  (SCI-unimpaired forelimb) contralateral to the injections. Error bars indicate S.E.M.
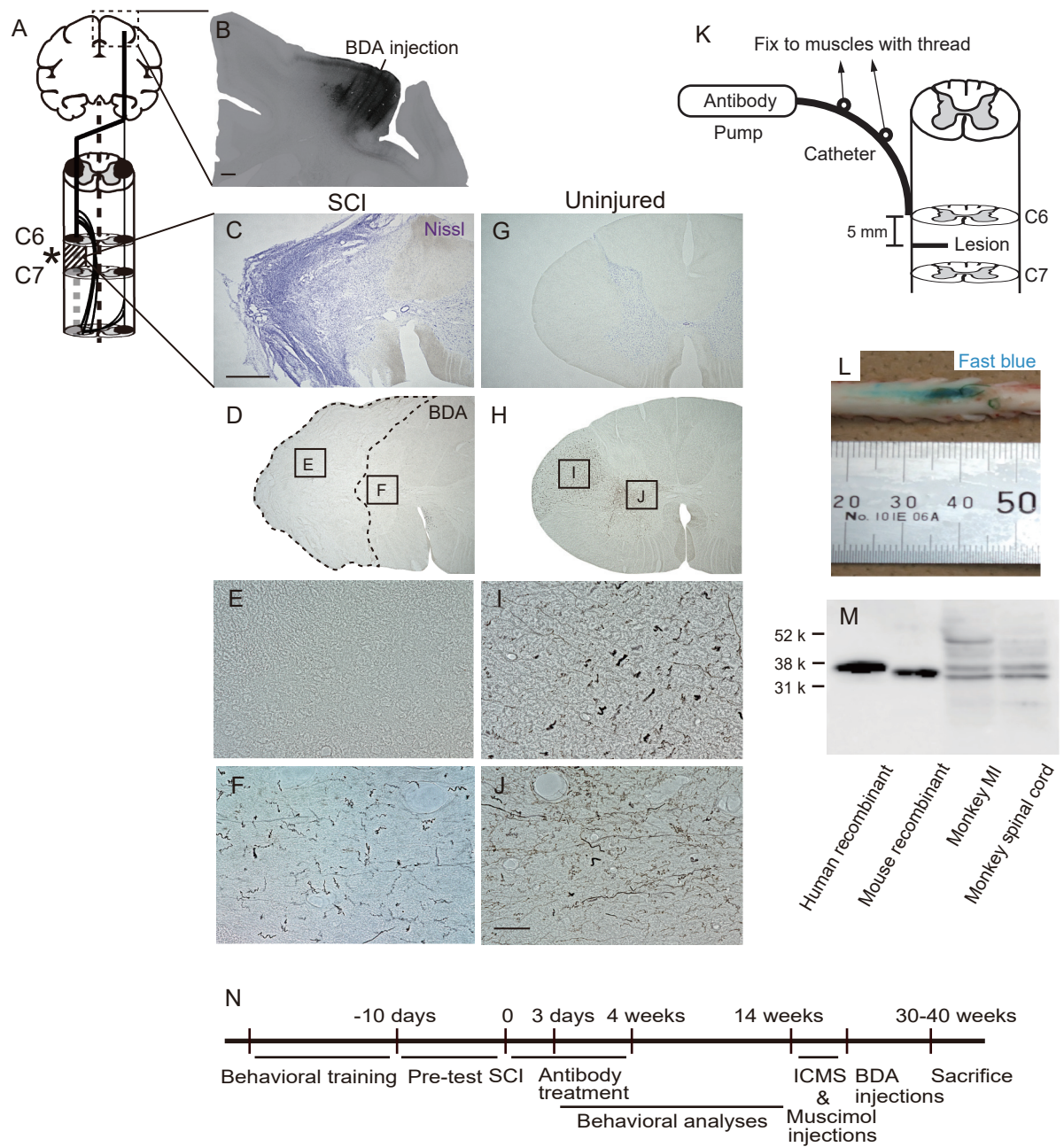
858  (Student's *t*-test, *$P < 0.05$).

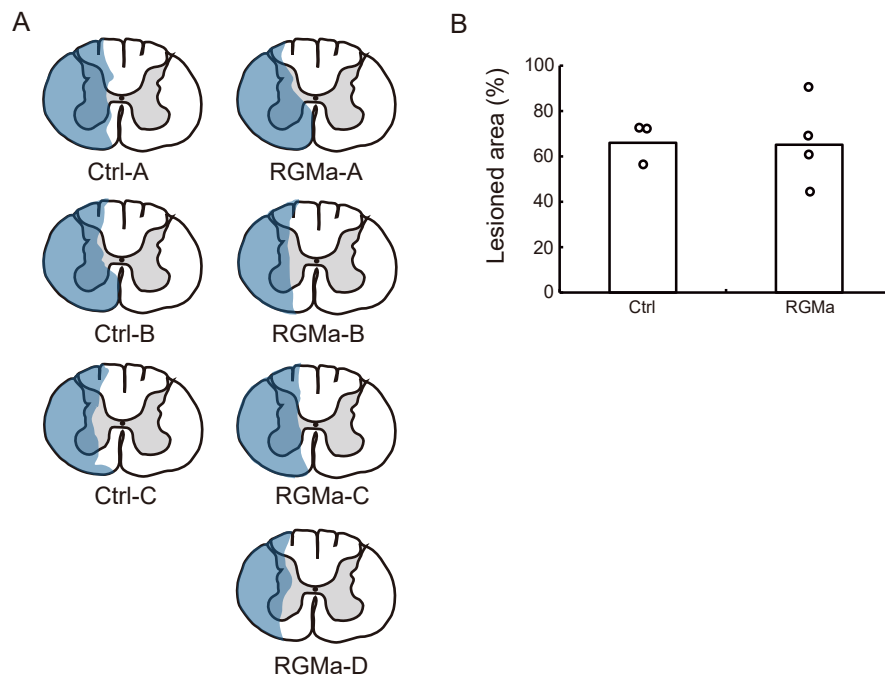A

B    BDA injection

SCI    Uninjured

C    Nissl    G

D    BDA    H
E    F    I    J

E    I

F    J

K    Fix to muscles with thread

Antibody Pump    Catheter

5 mm    Lesion

C6
C7

L    Fast blue

20    30    40    50
No. 101E 06A

M
52 k
38 k
31 k

Human recombinant
Mouse recombinant
Monkey MI
Monkey spinal cord

N

-10 days    0    3 days    4 weeks    14 weeks    30-40 weeks

Behavioral training    Pre-test SCI    Antibody treatment    ICMS & Muscimol injections    BDA injections    Sacrifice

Behavioral analyses

Figure 1
Nakagawa et al.

A

Ctrl-A    RGMa-A

Ctrl-B    RGMa-B

Ctrl-C    RGMa-C

RGMa-D
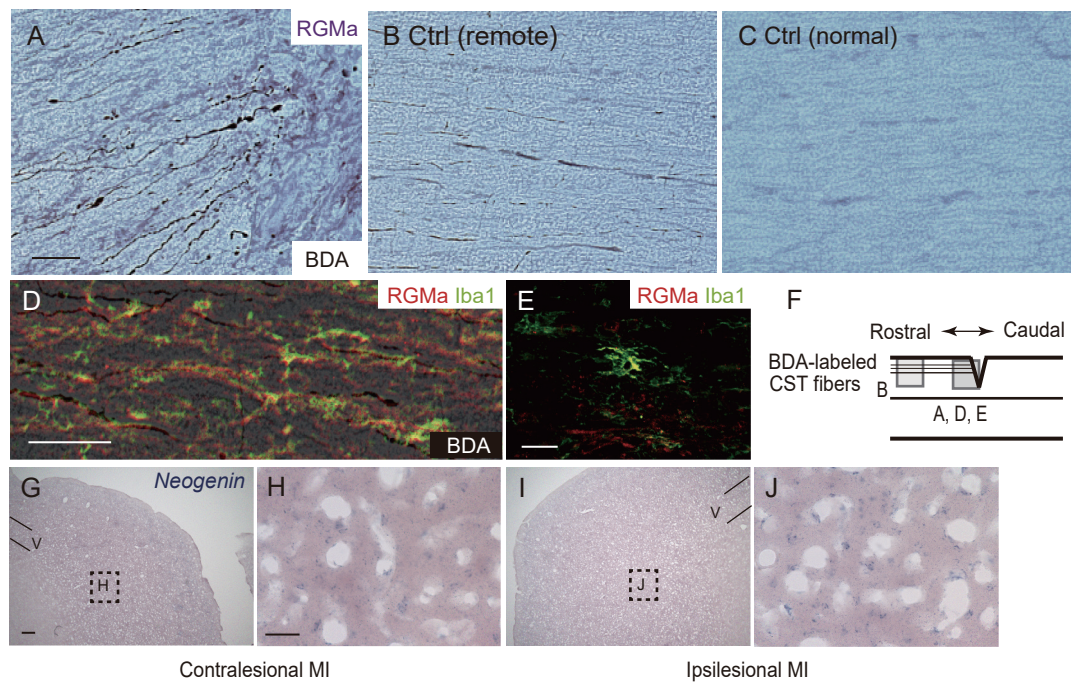
B



Figure 2

Nakagawa et al.
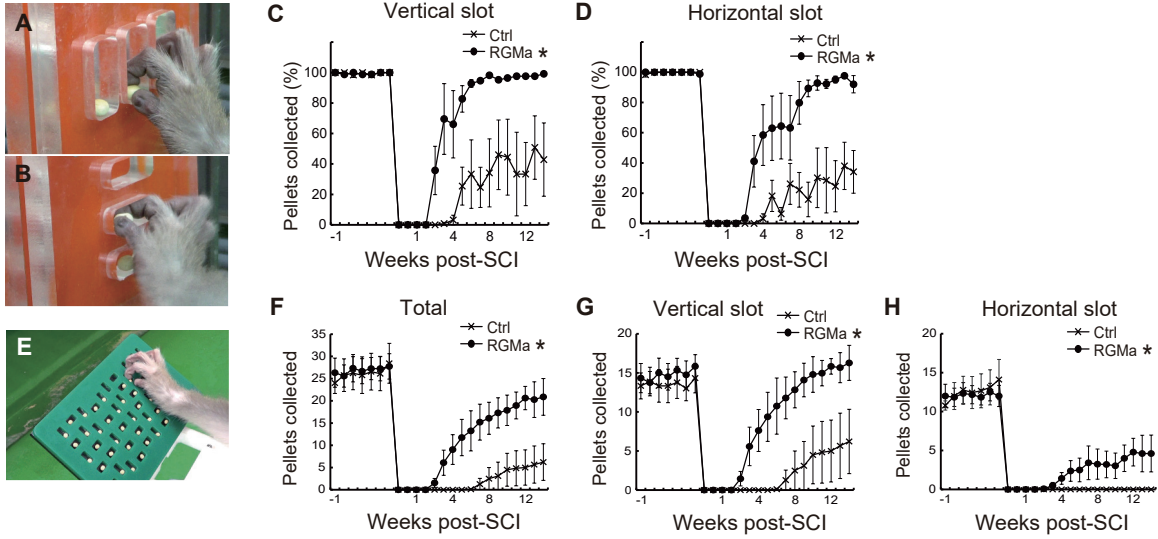
Figure 3

Nakagawa et al.
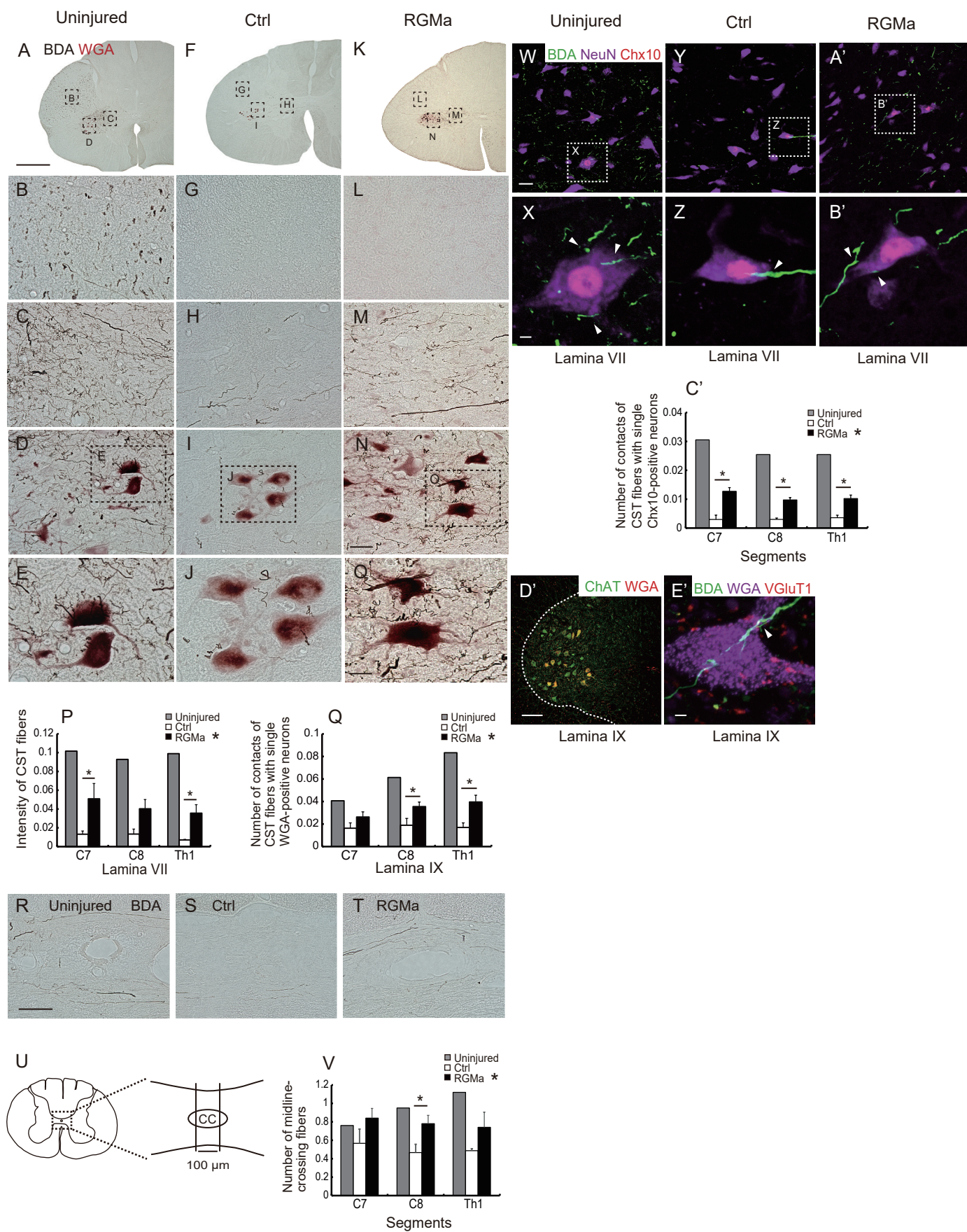
Figure 4
Nakagawa et al.

Figure 5
Nakagawa et al.

1 **Supplementary material**

2 **Treatment with the neutralizing antibody against repulsive guidance molecule-a**

3 **promotes recovery from impaired manual dexterity in a primate model of spinal**

4 **cord injury**

5 Hiroshi Nakagawa[1,2], Taihei Ninomiya[1], Toshihide Yamashita[2], Masahiko Takada[1]

6

7 [1]Systems Neuroscience Section, Primate Research Institute, Kyoto University.

8 [2]Department of Molecular Neuroscience, Graduate School of Medicine, Osaka

9 University.

10

11     **Video S1.** Recovery process of the reaching/grasping task performance in a control

12     antibody-treated and an anti-RGMa antibody-treated monkey. Fourteen weeks after SCI,

13     the control antibody-treated monkey can manage to take out pellets from vertical and

14     horizontal slots mainly using a power grip. On the other hand, the anti-RGMa

15     antibody-treated monkey can take out at least some pellets from both types of the slots

16     skillfully using a precision grip.

17

18     **Video S2.** Recovery process of the modified Brinkman board test performance in a

19     control antibody-treated and an anti-RGMa antibody-treated monkey. This movie shows

20     that the monkeys take out pellets before, 3 days, and 14 weeks after SCI. Before SCI,

21     the monkeys smoothly take out pellets from both the vertical and the horizontal slots.

22     Just after SCI, the monkeys cannot take out any pellet at all. Fourteen weeks after SCI,

23     the control antibody-treated monkey can take out some pellets only from the vertical

24     slots. On the other hand, the anti-RGMa antibody-treated monkey can take out pellets

25     not only from the vertical slots, but also from the horizontal slots.